leads to badly converging refinements if $\alpha > 0$ or the shifts of β or β itself are large ($\alpha > 0$).

One can try to remove this difficulty by using **g** as a constant, which is calculated only once at the beginning of a refinement. This cannot be recommended because it corresponds to an increase of (at most) six parameters for each atom. A procedure which refines first the harmonic parameters for $\alpha = 0$ and then the anharmonic parameters with β = constant can be used. But in the end all parameters must be refined together.

References

BACHMANN, R., KREUER, K. D., RABENAU, A. & SCHULZ, H. (1981) Conference on Chemistry and Physics of Sulfides, Selenides and Tellurium in Solids. Collected Abstracts.

CAVA, R. J., REIDINGER, F. & WUENSCH, B. J. (1980). *Solid State Commun.* **24**, 411–416.

EDGEWORTH, F. Y. (1905). *Proc. Cambridge Philos. Soc.* **20**, 36–141.

HOSHINO, S. & SAKUMA. T. (1980). *J. Phys. Soc. Jpn.* **48**, 1036.

International Tables for X-ray Crystallography (1974). Vol. IV. Birmingham: Kynoch Press.

JOHNSON, C. K. (1969). *Acta Cryst.* A**25**, 187–194.

JOHNSON, C. K. (1970). *Thermal Neutron Diffraction*, pp. 132–160. Oxford Univ. Press.

JOHNSON, C. K. (1980) *Thermal Motion Analysis*. Report 1980 DOE/TIC-11068. Oak Ridge National Laboratory, Oak Ridge, Tennessee.

MATSUBARA, T. (1975). *Prog. Theor. Phys.* **53**, 1210–1211.

PERENTHALER, E. & SCHULZ, H. (1981) *Solid State Ionics*, **1**, 335–365.

PERENTHALER, E., SCHULZ, H. & BEYELER, H. U. (1981) *Acta Cryst.* B**37**, 1017–1023.

SCHERINGER, C. (1977*a*). *Acta Cryst.* A**33**, 426–429.

SCHERINGER, C. (1977*b*). *Acta Cryst.* A**33**, 879–884.

SCHULZ, H., PERENTHALER, E. & ZUCKER, U. H. (1982). *Acta Cryst.* A. In the press.

WALLACE, D. L. (1958). *Ann. Math. Stat.* **29**, 635–654.

WILLIS, B. T. M. (1969). *Acta Cryst.* A**25**, 277–300.

WILLIS, B. T. M. & PRYOR, A. W. (1975). *Thermal Vibrations in Crystallography*. Cambridge Univ. Press.

ZUCKER, U. H., PERENTHALER, E., KUHS, W. F., BACHMANN, R. & SCHULZ, H. (1982). *PROMETHEUS*. Program system for structure refinements. Submitted to *J. Appl. Cryst.*

ZUCKER, U. H. & SCHULZ, H. (1982). *Acta Cryst.* (1982). A**38**, 568–576.

Acta Cryst. (1982). A**38**, 568–576

Statistical Approaches for the Treatment of Anharmonic Motion in Crystals. II. Anharmonic Thermal Vibrations and Effective Atomic Potentials in the Fast Ionic Conductor Lithium Nitride (Li_3N)

BY UDO H. ZUCKER AND HEINZ SCHULZ

Max-Planck-Institut für Festkörperforschung, Heisenbergstrasse 1, *D*-7 *Stuttgart* 80, *Federal Republic of Germany*

(*Received* 24 *June* 1981; *accepted* 22 *December* 1981)

Abstract

Results of X-ray diffraction experiments on lithium nitride (Li_3N) in the temperature range between 294 and 888 K show strong anharmonic effects. The deviations from harmonicity cannot be interpreted by interstitial sites or split positions. The application of an anharmonic temperature factor which is based on the Gram–Charlier expansion leads to an excellent fit of the data, whereas an anharmonic temperature factor, based on the Edgeworth series expansion, cannot fit the measurements in a satisfactory way. The corresponding anharmonic probability densities and the effective one-particle potentials are presented. The activation energy of the ionic conduction in Li_3N perpendicular to the c axis and the thermal expansion of the lattice constant are derived from the potentials. These results agree well with results obtained by other experimental techniques. Therefore it is concluded that the potentials derived from elastic scattering experiments are physically meaningful.

0567-7394/82/050568-09$01.00

1. Introduction

The most commonly used structure factor formalisms for the treatment of anharmonic thermal motion in crystals has been discussed in part I (Zucker & Schulz,

1982). For general applications we prefer the formalism based on the Gram–Charlier series. This formalism can be used for all site symmetries and in each oblique crystal coordinate system. The corresponding probability density function and the effective one-particle potential can be calculated exactly and evaluated numerically.

In this paper we describe the investigation of the fast ionic conductor Li_3N with X-ray diffraction. The investigations were carried out to check if the anharmonic potentials derived from elastic scattering experiments are physically meaningful. Li_3N was chosen for these investigations because of its simple crystal structure and its high ionic conductivity.

Lithium nitride crystallizes in the hexagonal space group $P6/mmm$ with $a = 3{\cdot}65$ and $c = 3{\cdot}88$ Å (at room temperature). The nitrogen atoms occupy the centre of the elementary cell (Fig. 1). They are surrounded by eight lithium atoms in the shape of a hexagonal bipyramid (Zintl & Brauer, 1935; Rabenau & Schulz, 1976). Several investigations (Schulz & Schwarz, 1978; Pattison & Schneider, 1980; Kerker, 1981) have shown that Li_3N forms ionic bonds; its valence formula can be written therefore as $Li_2^+N^{3-}$.

The large Li conductivity of Li_3N (Boukamp & Huggins, 1976; von Alpen, Rabenau & Talat, 1977) suggested a high degree of positional Li disorder. X-ray investigations from 153 up to 678 K (Schulz & Thiemann, 1979) were carried out to determine the conduction paths in Li_3N. The obtained difference electron densities using anisotropic temperature factors showed remarkable densities in the Li_3N plane ($z = 0$). Schulz & Thiemann (1979) concluded therefore that the high ionic conductivity is caused by jumps of the Li(2) ions (Fig. 1), where the precursors of these jumps are anharmonic thermal vibrations. No interstitial sites should be involved in this mechanism.

Li_3N therefore seemed to be well suited for testing models of anharmonic motion. In addition, the simple crystal structure of Li_3N allows a comparison between refined potentials and macroscopic parameters.

Measurements were carried out up to a temperature of 888 K, because of the low occupation of high-energy states at room temperature. Temperatures above 700 K were needed to activate a measurable fraction of the lithium ions to energy states above the activation energy of 0·29 eV. (This is the activation energy of the ionic conductivity perpendicular to the c axis; an appreciable occupation of energy states above the activation energy parallel to **c** of 0·5 eV will not be obtained because of the melting point of 1086 K.)

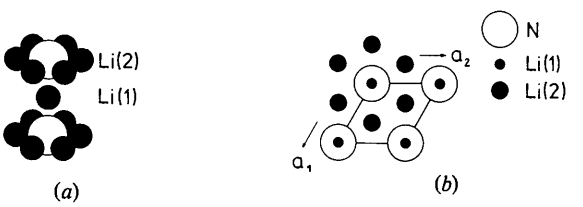

Fig. 1. Crystal structure of Li_3N. (*a*) Perspective drawing; (*b*) projection along **c**.

2. Experimental

A single crystal of roughly spherical shape and about 250 μm in diameter was taken from a large single crystal grown by the Czochralski technique (Schönherr, Müller & Winkler, 1978). The crystal was put into a tube of Lindemann glass to prevent reaction with the air. The use of quartz glass was impossible because Li_3N reacts with quartz glass above 650 K. The tube of Lindemann glass was mechanically stabilized by fixing it in a tube of quartz glass (Lindemann glass becomes soft above 700 K).

Data collection was carried out at nine different temperatures between 294 and 888 K. Above 900 K the Lindemann glass becomes too soft to fix the crystal. All measurements were done on a Philips single-crystal four-circle diffractometer PW1100, using monochromatized Mo $K\alpha$ radiation. The crystal was heated in a stream of hot air. The temperature was measured with a Cr–Ni thermocouple within a precision of 5 K (10 K) up to (above) 670 K. In order to minimize the influence of diffuse scattering from the glass tubes ω scans were used. At all but the highest temperatures about 690 reflections were measured (using the background–peak–background method). The reflections are given by h arbitrary, k, $l \geq 0$, $\sin\theta/\lambda \leq 0{\cdot}9$ Å^{-1} and their Friedel reflections.

At 888 K only 80% of these data were measured with the additional condition $l < 6$. This set of data is incomplete because the crystal was destroyed during the measurement. The crystal reacted rapidly with the quartz glass at the end of the measurement. The first 80% of the data set are not influenced by this process, judging from the measurement of the control reflections.

The absorption could be neglected because $\mu r = 0{\cdot}06$ for the crystal. The errors of the mean intensity $\bar{I}$ for a group of at least six symmetry-equivalent reflections was calculated from the counting statistics and from the deviations of the single measurements from the mean. The larger value was then taken as $\sigma(\bar{I})$. Now the curve $\sigma(\bar{I})$ as a function of $\bar{I}$ was used to estimate the errors of those $\bar{I}$ which were calculated from less than six single intensity measurements. These errors were used to calculate the weights for the least-squares refinements.

The intensities were corrected for thermal diffuse scattering of first order using the method of Skelton & Katz (1969). The elastic constants except c_{13} were taken from Kress, Grimm, Press & Lefebevre (1981).

The constant c_{13} has not been measured so far because of experimental problems (cleavability). Therefore we used as an approximation $c_{13} \simeq 18$ Tg m^{-1} s^{-2}, which was calculated from the lattice dynamical model of Li_3N (Chandrasekhar, Bhattachary, Migoni & Bilz, 1978).

All data were corrected for extinction using the formalism of Becker & Coppens (1974). The best results were obtained with the extinction type I, Gaussian distribution. The differences to the other types, however, are rather small. No difference within their errors was found between the Zachariasen (1967) and the Becker & Coppens (1974) correction (type I, Gaussian), because of the small extinction effects in Li_3N [$y \geq 0{\cdot}85$, where $I(\text{obs}) = yI(\text{calc})$].

3. The simple harmonic model of lithium nitride

Fig. 2 shows the variation of the lattice constants with temperature in the range between 10 and 888 K. The measurements at 10 K were carried out by Heger (1979) using neutrons and those at 153 K by Schulz & Thiemann (1979) using X-rays.

Apart from a slight increase at moderate temperatures, the c-axis constant is nearly constant within its error. The a-axis constant, in contrast, shows a marked increase with temperature. Below 273 K this increase is linear. Above room temperature, however, it varies rapidly until it tends to a saturation value above 820 K.

The a-axis constant shows large deviations from a simple harmonic model. Such a model predicts (in combination with the assumption of isolated atoms) that the variations of the lattice constants are zero. Similar deviations can also be observed in the development of the reliability factor R_w (Fig. 3) for refinements using the conventional structure factor equation, as well as in the mean-square displacements (Fig. 4). [We emphasize that these displacements differ from linearity (predicted by the harmonic model) both to smaller and to larger values.]

The largest deviations from a harmonic structure model can be deduced from a difference electron density. They are drawn for four selected temperatures in Fig. 5 for the Li_2N ($z = 0$) plane and in Fig. 6 for the plane shown in Fig. 6(e). All figures point to residual densities mainly around the Li(2) position. These densities increase considerably with increasing temperature. They are significantly higher than their errors, which are calculated to about 0·04 e Å^{-3} and which are restricted to small areas in the vicinity of the atom sites only. The difference electron densities around the Li(2) positions correspond to a strong decrease of the occupation probability of Li(2) (Fig. 7), whereas the occupation of the Li(1) remains nearly constant.

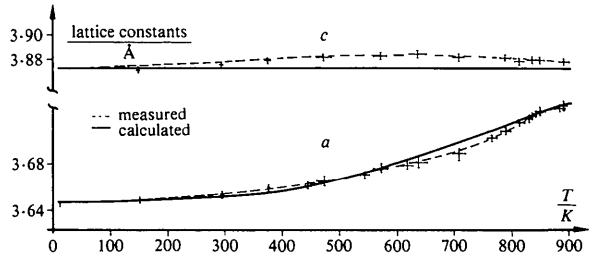

Fig. 2. Thermal lattice expansion as a function of the temperature given by measurement and by model calculation.

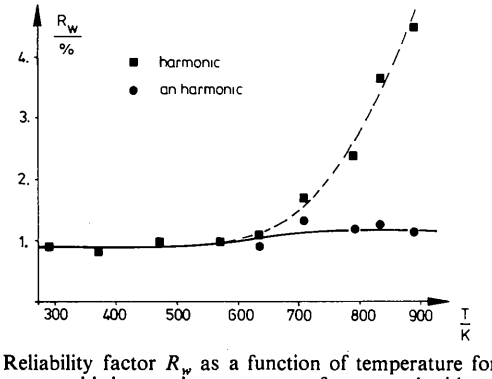

Fig. 3. Reliability factor R_w as a function of temperature for the refinements with harmonic temperature factors and with anharmonic temperature factors based on the Gram–Charlier expansion.

4. Interstitial-site and split-atom models

For the moment we restrict ourselves to the data measured at 888 K, because they have the largest deviations from the simple harmonic model. Table 1 shows the reliability factors R, R_w and the goodness of fit of an interstitial-site model [the ions lost from the Li(2) positions generate Frenkel defects at $\frac{1}{2},\frac{1}{2},0$], a split-atom model [Li(2) ions at $x,2x,0$] and the simple harmonic model.

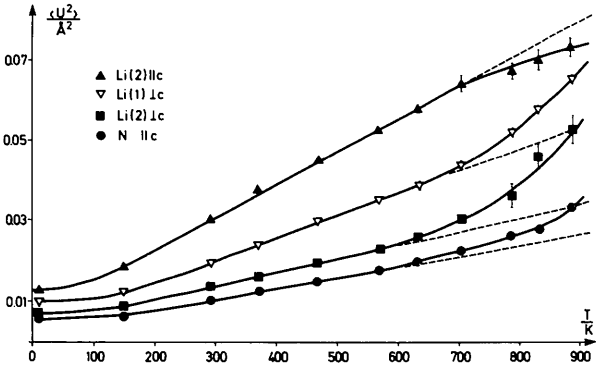

Fig. 4. Mean-square displacements refined for Li_3N with harmonic temperature factors. The differences between $\langle u^2\rangle_{N\parallel c}$, $\langle u^2\rangle_{N\perp c}$ and $\langle u^2\rangle_{Li(1)\cdot c}$ are negligible and therefore only $\langle u^2\rangle_{N\parallel c}$ is drawn. The values at 153 K are from Schulz & Schwarz (1978), the values at 10 K from Heger (1979).

The refined occupation probability of the interstitial site is 0·075 (1). Added to the occupation of the Li(2) site one gets an overall occupation, which is a little less than the value refined at 294 K. However, the thermal vibrational amplitude of the interstitial site is equal to 0·27 Å. The coordinate of the split-atom model is $x = 0{\cdot}354$ (5), the sum of the occupation probabilities of three symmetrically equivalent Li(2) split positions equals 0·90 (3).

The split-atom model can be rejected because of the high residual electron density (Fig. 8*b*) and the slight decrease of the reliability factors. The interstitial-site model leads to a significant decrease of the R values. However, the model has to be rejected, because of the following.

(1) The corresponding difference electron density (Fig. 8*a*) shows a density with threefold symmetry around the Li(2) site, which points to an undescribed antisymmetric part of thermal vibrations or to a split position.

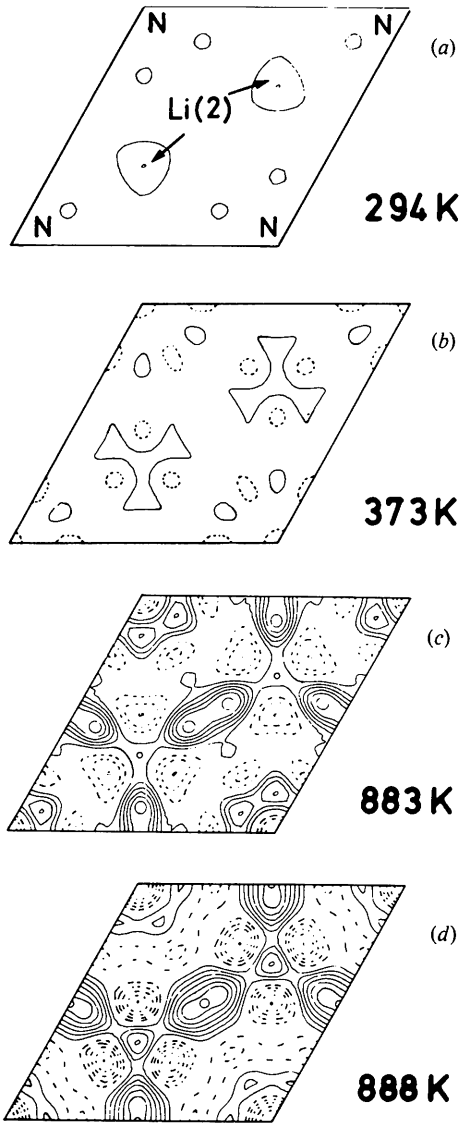

Fig. 5. Difference electron densities of the harmonic model in the Li_2N ($z = 0$) plane as a function of temperature. Lines $\pm 0{\cdot}03$, $\pm 0{\cdot}06$, ... e Å^{-3}. —— Positive; – – – negative.

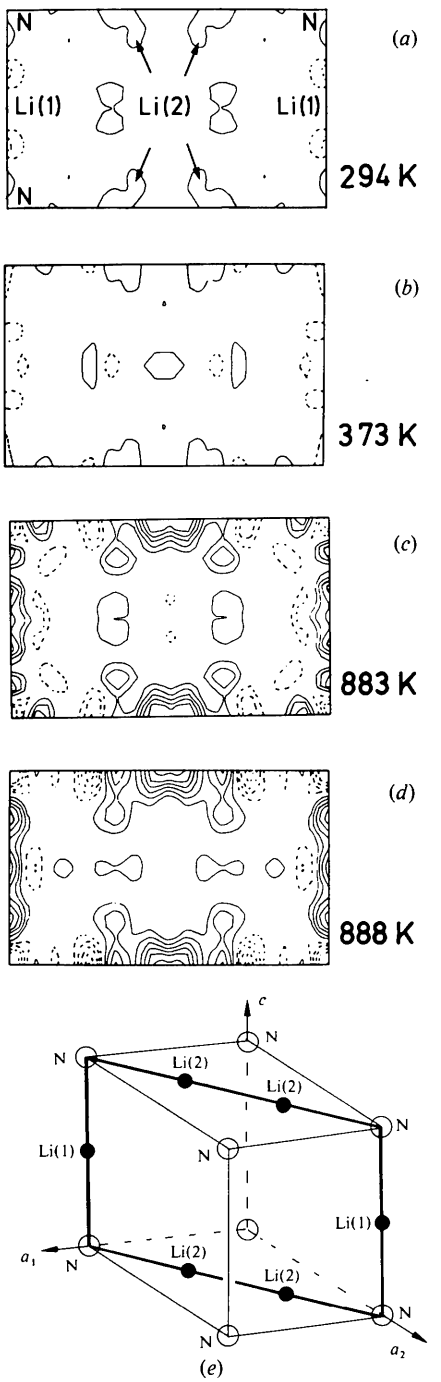

Fig. 6. Difference electron densities in the plane described in Fig. 6(*e*) as a function of temperature. Lines as in Fig. 5.

Table 1. *Refinements with harmonic temperature factors for the* 888 K *data*

Model	R (%)	R_w (%)	Goodness of fit	Number of parameters
Interstitial sites	2·7	2·5	2·3	11
Split atom	3·4	2·9	2·9	11
Simple harmonic	4·5	3·8	3·8	10

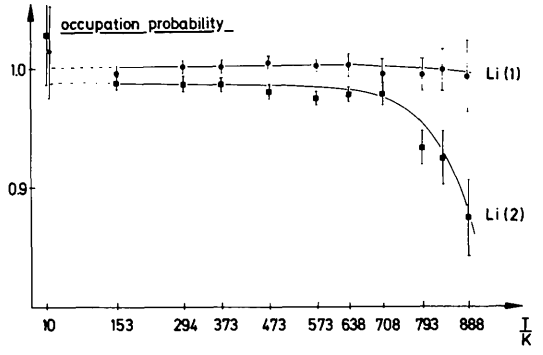

Fig. 7. Occupation probability of the lithium ions from refinements with harmonic temperature factors. Data at 10 K from refinements with neutrons (Heger, 1979).

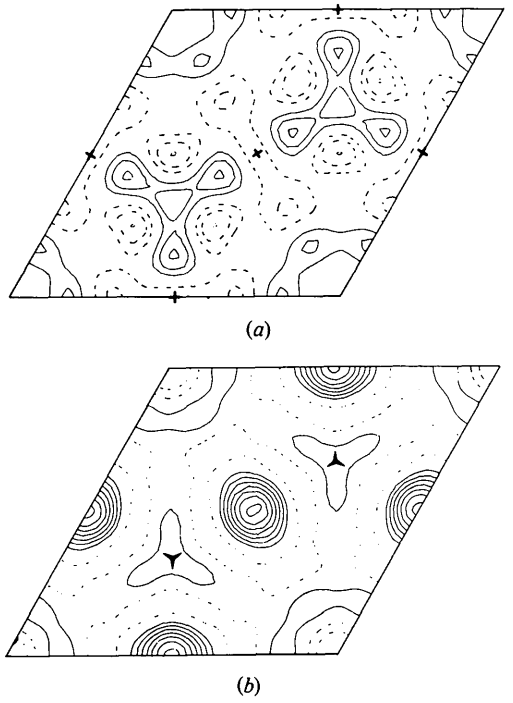

Fig. 8. Difference electron density of Li_3N (888 K) refined in an interstitial site model (*a*) and in a split-atom model (*b*). The crosses in (*a*) mark the interstitial sites. The threefold axis symbols in (*b*) mark the split positions. Lines as in Fig. 5.

(2) The distance between two neighbouring Li(2) ions is too short to insert an additional ion between them.

(3) The electron density shows a minimum at the position of the interstitial site and therefore we expect a maximum of the potential at $(\frac{1}{2},\frac{1}{2},0)$.

5. Anharmonic thermal vibrations in Li_3N

We applied several structure factor equations for anharmonic thermal motion to the data measured at 888 K to investigate differences between these models. The results are given in Table 2.

The residual density of the Edgeworth expansion (Fig. 9*a*) is similar to that of Fig. 8(*b*) and, by using a

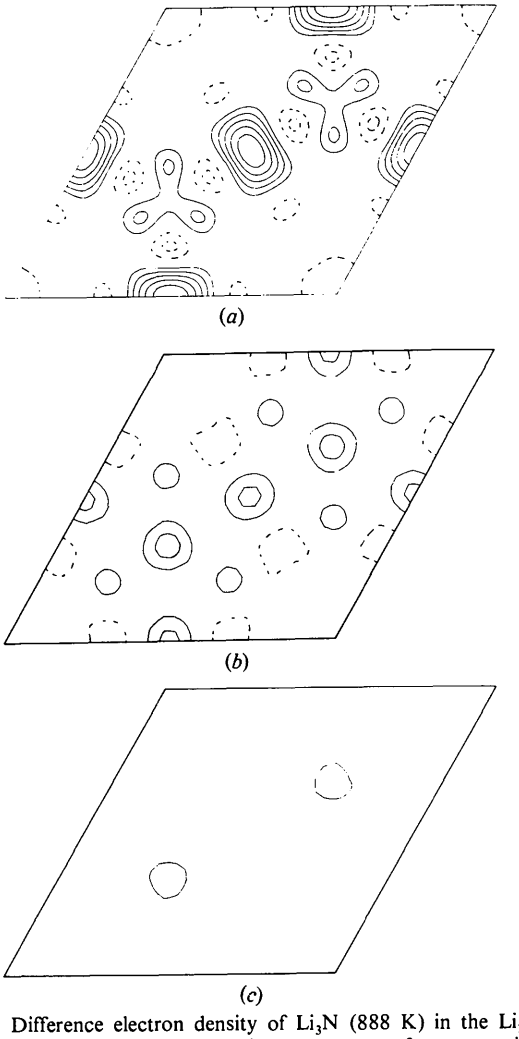

Fig. 9. Difference electron density of Li_3N (888 K) in the Li_2N plane. Results of refinements using the structure factor equation based on: (*a*) the Edgeworth expansion up to fourth-rank tensors; (*b*) the Gram–Charlier expansion up to fourth-rank tensors; (*c*) the Gram–Charlier expansion up to sixth-rank tensors for Li(2), up to fourth-rank tensors for Li(1) and N. Lines as in Fig. 5.

Table 2. *Refinements with anharmonic temperature factors for the* 888 K *data*

Model*	R (%)	R_w (%)	Goodness of fit	Number of parameters	Occupation of Li(2)	Difference electron density
Edgeworth expansion up to fourth order	2·7	2·6	2·6	19	0·93 (1)	Fig 9(*a*)
Gram–Charlier expansion up to fourth order	1·5	1·5	1·4	19	0·98 (1)	Fig. 9(*b*)
Gram–Charlier expansion up to sixth order	1·1	1·15	1·0	19†	0·98 (1)	Fig. 9(*c*)

* The occupation of Li(1) was fixed. Its value did not differ significantly from 1 when refined in the anharmonic models. The reliability factors did not change.

† All insignificant parameters were fixed in an iterative way to zero (described in Schulz, Perenthaler & Zucker, 1982) so that the number of independent parameters were reduced from 27 to 19.

Table 3. *Results of the structure refinement with the Gram–Charlier expansion for the* 833 K *data*

The temperature factor equation is listed in part I.

Scale factor	79·7 (6)		
Extinction	0·23 (3)	Mosaic spread	25·7″
Thermal parameters			
N	β_{11}	0·0619 (14)	
	β_{33}	0·0392 (12)	
	d_{1111}	$(2·68 \pm 1·07) \times 10^{-6}$	
	d_{3333}	$(2·12 \pm 0·79) \times 10^{-6}$	
Li(1)	β_{11}	0·114 (4)	
	β_{33}	0·0391 (11)	
	d_{1111}	$(11·8 \pm 5·2) \times 10^{-6}$	
Li(2)	β_{11}	0·136 (9)	
	β_{33}	0·101 (3)	
	c_{111}	$-(2·7 \pm 0·3) \times 10^{-4}$	
	d_{1111}	$(99·4 \pm 22·0) \times 10^{-6}$	
	e_{11111}	$-(4·8 \pm 1·5) \times 10^{-6}$	
	f_{111111}	$(1·7 \pm 0·4) \times 10^{-6}$	
	f_{333333}	$-(0·2 \pm 0·1) \times 10^{-6}$	
	f_{111122}	$(0·05 \pm 0·14) \times 10^{-6}$	
	f_{113333}	$-(0·09 \pm 0·05) \times 10^{-6}$	
Occupation probability of Li(2)		0·98 (1)	

statistical test only, we have to reject this anharmonic model compared to the interstitial-site model.

The structure factor equation based on the Gram–Charlier expansion improves the refinement considerably. The resulting difference electron density (Fig. 9*c*) is nearly equal to the residual density at 294 K and the occupation of the Li(2) site is equal to the value refined at 294 K. The final structure parameters are listed in Table 3.

The application of this model to all nine sets of data* [reduced to significant parameters for each temperature (ten up to 573 K, 11 for 638 K, 16 for 793 K and 19 for 883 K and 888 K)] leads to a crystal structure model of Li_3N which is excellently consistent in the entire temperature range of our measurements. The reliability factor R_w (Fig. 3) is nearly constant and it is equal to the value refined at room temperature. From Fig. 10 we conclude that the decrease of the occupation probability of Li(2) (Fig. 7) is mainly caused by uncovered parts of the electron density in the harmonic model and not by Frenkel defects.

6. Anharmonic-effective one-particle potentials

From the anharmonic temperature factors we can derive a probability density (Fig. 11) and an effective one-particle potential (Zucker & Schulz, 1982).

In order to check the physical significance of the refined potential, it has to be calculated for each set of data. If the potential is nearly independent of temperature, we can conclude that our refinements are physically meaningful. Interpreting potentials like that in Fig. 13, one has to take into account the occupation of the energy states. At low temperatures only a few atoms have a high energy and hence the potential is not well determined at points far away from the equilibrium position. The reliability of such parts of the potential improves with increasing temperature. A rough estimation of the occupation can be given by the

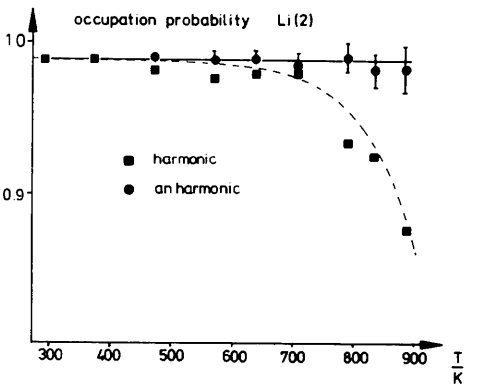

Fig. 10. Occupation probability of Li(2) in the harmonic and the anharmonic structure model. (Gram–Charlier.)

* Lists of structure factors for all data sets have been deposited with the British Library Lending Division as Supplementary Publication No. SUP 36618 (19 pp.). Copies may be obtained through The Executive Secretary, International Union of Crystallography, 5 Abbey Square, Chester CH1 2HU, England.

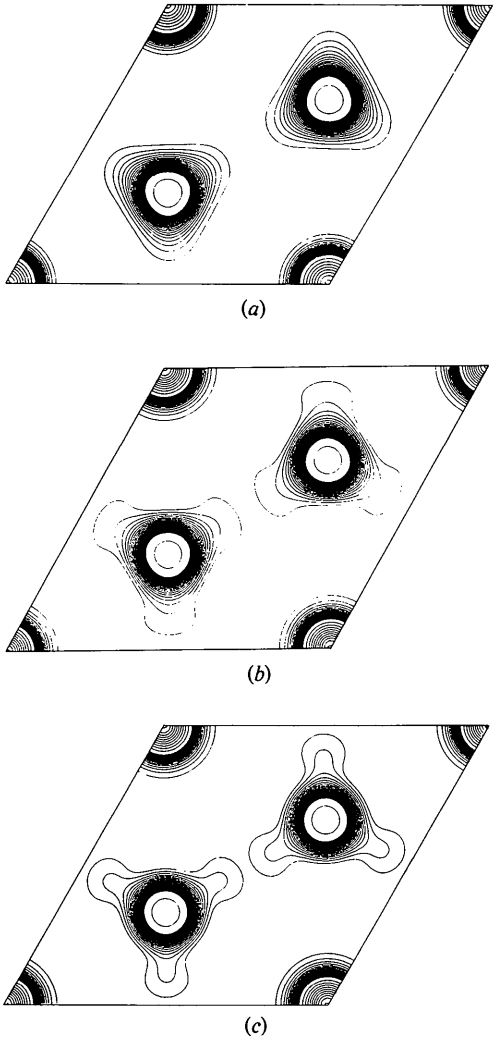

Fig. 11. Probability density maps in the Li_2N plane (888 K) calculated from (*a*) the Edgeworth and (*b*), (*c*) the Gram–Charlier expansion. (*a*), (*b*) Up to fourth-rank tensors, (*c*) up to sixth-rank tensors. Lines 5, 10, 15, ..., 100, 150, ... $Å^{-3}$.

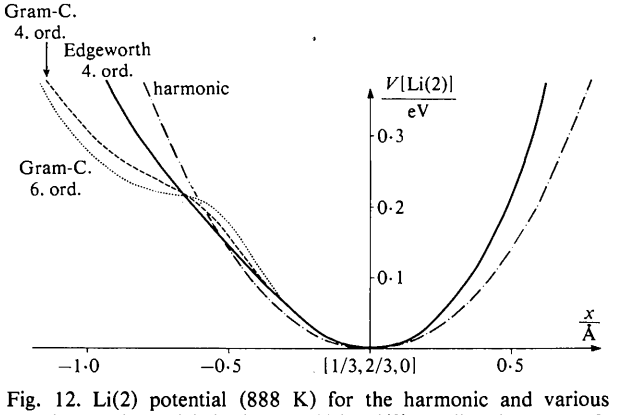

Fig. 12. Li(2) potential (888 K) for the harmonic and various anharmonic models in the N–Li(2)–Li(2)–N direction at $z = 0$. The results of all anharmonic potentials are identical at the right side of the drawing (Li–N bond).

Bose–Einstein distribution. This distribution, however, is only valid for a parabolic, *i.e.* harmonic, potential and in the case of a flat potential it leads to an overestimation.

The potential considered here is that of the Li(2) ion in the N–Li(2)–Li(2)–N direction (Fig. 12), where we find the largest deviations from a parabolic (harmonic) potential. In Fig. 12 this potential is drawn for the different anharmonic models, in Fig. 13 it is given as a function of temperature. (For the Edgeworth expansion we have only drawn the results of the normal Edgeworth approximation.)*

The potential derived from the Gram–Charlier expansion of fourth and sixth order is a consistent improvement of the potential of the Edgeworth series. All anharmonic models give the same result in the direction towards the N^{3-} ion, whereas in the opposite direction the different models lead to different potential forms. Compared to the Edgeworth expansion the Gram–Charlier series leads to a more detailed potential form. From the refined potentials we conclude a strongly repulsive interaction towards the N^{3-} ion, probably dominated by the exchange and Coulomb interactions of the electron clouds of Li(2) and N^{3-}. Compared with these interactions the interaction between neighbouring $Li(2)^+$ ions seems to be reduced by the smeared electron density (in the outer-range) of the N^{3-} ion, which behaves like a dielectric. The approach of two Li(2) ions, however, is limited by the Coulomb repulsion.

A comparison of the harmonic potential with the anharmonic potentials explains the negative and positive residual densities in Fig. 5(*d*). The anharmonic

* The difference between the results of the normal and the extended approximation (Zucker & Schulz, 1982) is at most 13·5% at the position of the Li(2) ion. The corresponding potential of the extended approximation is somewhat flatter in the Li(2) direction than the potential of the normal approximation.

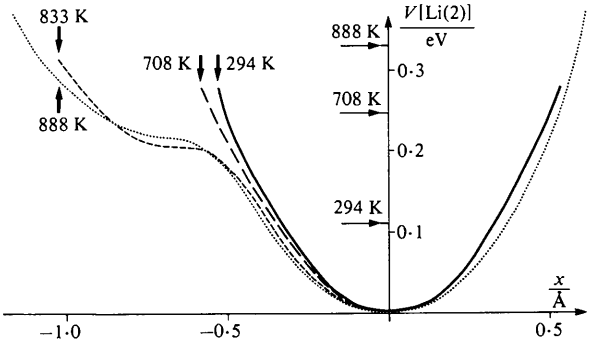

Fig. 13. Li(2) potential in the anharmonic model using the Gram–Charlier expansion in the N–Li(2)–Li(2)–N direction at $z = 0$, for different temperatures. All results on the right side are identical for temperatures below and above 700 K, respectively. In addition the occupation probability 0·01 calculated from the Bose–Einstein distribution is shown by the horizontal arrows.

potentials are steeper than the harmonic potentials in the directions Li–N. Therefore the harmonic potential generates too much density in this direction and this shows up in the difference densities as a negative residual density. The opposite arguments are true for the direction Li–Li.

Because of the above arguments, in Fig. 13 one can only compare those parts of the potentials for which the energy states are sufficiently occupied at different temperatures. In Fig. 13 we have marked the energies where the Bose–Einstein distribution gives an occupation of 0·01. At 888 K we therefore can estimate the potential at the midpoint between two Li(2) ions with good accuracy.

Up to 700 K all potentials are nearly identical, therefore we have only drawn that for 294 K.

7. Macroscopic quantities derived from the potential

In Fig. 14 we have drawn the potential of the refinement using the Gram–Charlier expansion up to sixth order for two neighbouring Li(2) ions, where we have interpolated the potentials in the region of overlap. This interpolation is of course not unique. We have therefore assumed an error of about 0·04 eV. The height of the barrier between the atom sites is about 0·29 (4) eV. If we interpret the ionic conduction mechanism of the Li^+ perpendicular to the c axis as a hopping process over this potential barrier, the conductivity must follow an Arrhenius law and the activation energy must be between 0·25 and 0·33 eV. Both conclusions are in agreement with the results reported by von Alpen *et al.* (1977), who measured an activation energy of 0·29 eV using electrical methods.

In addition we have calculated the expansion of the lattice constants using the Li(2) potential (Appendix). The results are shown in Fig. 2. The main features of the thermal expansion are reproduced; the remaining deviations can be explained by the temperature dependence of the potential above 700 K. The good agreement between experimental and calculated thermal expansion is a convincing argument that the potentials derived from elastic scattering experiments are physically meaningful.

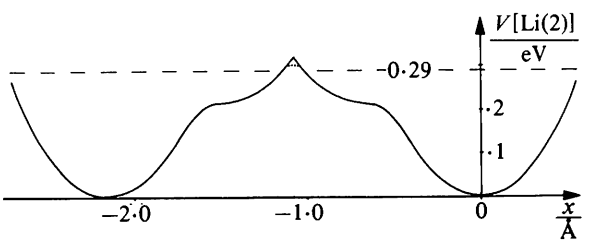

Fig. 14. Potential between two neighbouring Li(2) ions at 888 K (Gram–Charlier up to sixth rank). It is interpolated in the region of overlap.

All calculations were carried out with the program system *PROMETHEUS* (Zucker, Perenthaler, Kuhs, Bachmann & Schulz, 1982) towards a neighbouring Li(2) ion. The change of the potential as a function of temperature cannot be caused by an incomplete correction of the thermal diffuse scattering.

In Fig. 15 we present the potential refined with the data measured at 888 K with and without corrections for the thermal diffuse scattering. The influence of the TDS is surprisingly small, although the maximum contribution of the TDS to the integrated intensity is 40%. The reason for this insensitivity is that the potential is a logarithmic function of the probability density (Zucker & Schulz, 1982). The result, derived for Li_3N, can be generalized to other substances, which do not show very strong anisotropic thermal diffuse scattering. Therefore the refinement of one-particle potentials can thus be meaningful in cases where it has so far not been possible to correct for TDS.

The authors are greatly indebted to Drs W. F. Kuhs and E. Perenthaler for their assistance in preparing this work.

APPENDIX
Calculation of the thermal expansion of Li_3N in a simple phenomenological model

The arrangement of the ions in Li_3N is given by the minimum of the free energy, which one cannot calculate in an easy way. Therefore a phenomenological model was used. For simplicity temperature-independent potentials were assumed.

With increasing temperature higher energy states are occupied. For every arbitrary direction the expectation value $\langle x \rangle_T$ of the position vector of a particle in the potential can be calculated. For centrosymmetric potentials we get a constant, whereas for acentric potentials we get a temperature-dependent value. In Li_3N only the Li(2) ion is in an acentric potential and has in this model an influence on the lattice expansion.

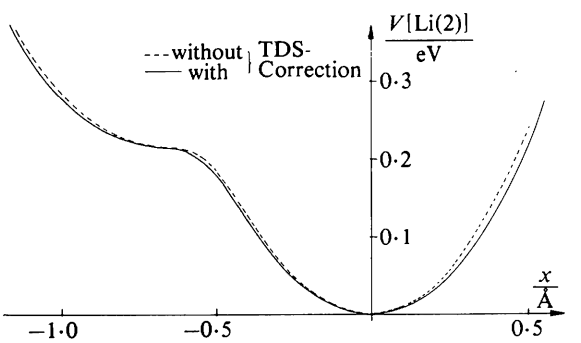

Fig. 15. Potentials of the Li(2) position (888 K) along the direction N–Li–Li–N at $z = 0$ with and without correction of thermal diffuse scattering. Gram–Charlier expansion up to sixth rank.

The Li(2) potential is not acentric in the c direction and therefore the c constant is independent of temperature (Fig. 2).

The a lattice constant can be changed by the Li(2) ions. To reduce the problem to a calculation in one dimension we make the assumption that the thermal lattice expansion is dominated by the approval of neighbouring Li(2) ions along the Li(2)–Li(2) direction.

The lattice constant at $T = 0$ K should be a_0, which is given to a good approximation by the a constant measured at 10 K. For each temperature the calculated a constant, $a_{calc}(T)$ must simultaneously fulfil the two equations

$$a_{calc}(T) = \frac{\sqrt{3}}{3}(\Delta d_{N,Li(2)} - \langle x\rangle_T)$$

and

$$a_{calc}(T) = \frac{\sqrt{3}}{3}(\Delta d_{Li(2),Li(2)} - 2\langle x\rangle_T),$$

where d_{AB} is the atomic distance between the ions A and B at temperature T and $\langle x\rangle$ is the mean of the location parameter of Li(2) (measured from $\frac{1}{3},\frac{2}{3},0$). $\langle x\rangle_T$ is calculated from the potential of the Li(2) ion refined at 833 K (parameters of this refinement are given above).

$$\langle x\rangle_T = \frac{\int_{-\infty}^{\infty} x \exp[V/(kT)]\,dx}{\int_{-\infty}^{\infty} \exp[-V/(kT)]\,dx}.$$

The relation between the atomic distances

$$d_{N,Li(2)} = S(T)\, d_{Li(2),Li(2)}$$

is simplified by the additional assumption that the scaling factor $S(T)$ is independent of temperature. This approximation is valid as long as $\langle x\rangle_T$ is small enough. We calculate S by minimizing the quadratic differences $[a_{measured}(T) - a_{calc}(T)]^2$ and get $s = 3{\cdot}37$. The corresponding $a_{calc}(T)$ is drawn in Fig. 2.

By interpreting the result of the a lattice constant of Fig. 2 one should keep in mind that the factor s is a scaling factor, which can only change the slope and does not influence the position of turning points and their sequence.

References

ALPEN, U. VON, RABENAU, A. & TALAT, G. H. (1977). *Appl. Phys. Lett.* **30**, 621–623.

BECKER, P. & COPPENS, P. (1974). *Acta Cryst.* A**30**, 129–147.

BOUKAMP, B. A. & HUGGINS, R. A. (1976). *Phys. Lett.* A**58**, 231–233.

CHANDRASEKHAR, H. R., BHATTACHARYA, G., MIGONI, R. & BILZ, H. (1978). *Phys. Rev. B*, **17**, 884–893.

HEGER, G. (1979). Private communication.

KERKER, G. (1981). *Phys. Rev. B*, **23**, 6312–6318.

KRESS, W., GRIMM, H., PRESS, W. & LEFEBVRE, J. (1980). *Phys. Rev. B*, **22**, 4620–4625.

PATTISON, P. & SCHNEIDER, J. R. (1980). *Acta Cryst.* A**36**, 390–398.

RABENAU, A. & SCHULZ, H. (1976). *J. Less-Common Met.* **50**, 155–159.

SCHÖNHERR, E., MÜLLER, G. & WINKLER, E. (1978). *J. Cryst. Growth*, **43**, 469–472.

SCHULZ, H., PERENTHALER, E. & ZUCKER, U. H. (1982). *Acta Cryst.* A. In the press.

SCHULZ, H. & SCHWARZ, K. (1978). *Acta Cryst.* A**34**, 999–1005.

SCHULZ, H. & THIEMANN, K. H. (1979). *Acta Cryst.* A**35**, 309–314.

SKELTON, E. F. & KATZ, J. L. (1969). *Acta Cryst.* A**25**, 319–329.

ZACHARIASEN, W. H. (1967). *Acta Cryst.* A**23**, 558–564.

ZINTL, E. & BRAUER, G. (1935). *Z. Elektrochem.* **41**, 102–107.

ZUCKER, U. H., PERENTHALER, E., KUHS, W. F., BACHMANN, R. & SCHULZ, H. (1982). *PROMETHEUS*. Program system for structure refinements. Submitted to *J. Appl. Cryst.*

ZUCKER, U. H. & SCHULZ, H. (1982). *Acta Cryst.* A**38**, 563–568.